Fluorescence Lifetime Imaging applied to the mixing between two non-isothermal sprays

M. Wang[1], M. Stiti[2], H. Chaynes[1], S. Becker[1], F. Lemoine[1], G. Castanet[1,*]

1: Université de Lorraine, CNRS, LEMTA, F-54000n Nancy, France

2: Division of Combustion Physics, Department of Physics, Lund University, Lund, Sweden

* Correspondent author: Guillaume.castanet@univ-lorraine.fr

Keywords: TCSPC, LIF, Spray Mixing, Temperature Imaging

ABSTRACT

Droplets temperature is a key parameter for the study of heat and mass transfers in many spray applications. In this study, we develop a new method based on the measurement of the fluorescence lifetime to characterize the droplet temperature in sprays. The method is tested in the mixing region of two water sprays, which are injected with a significantly different temperature. Time Correlated Single Photons (TCPSC) is applied to characterize the fluorescence decay in the time domain. For some well-chosen fluorescent dye, like rhodamine B (RhB), the fluorescence lifetime strongly varies with the temperature. Hence, in the mixing region of two non-isothermal sprays, the fluorescence of RhB is expected to follow a biexponential decay. In this study, we discuss the possibility of using this decay to determine the temperature of the two sprays as well as their respective volume fraction.

In a first step, a simplified configuration is considered where the two sprays are seeded with eosin Y and rhodamine 6G separately. Since these dyes have very different lifetimes and are not temperature dependant, the fluorescence decay changes with the mixing fraction alone. A calibration is necessary to evaluate the amount of liquid originating from each of the two sprays in the measurement volume. The femtosecond laser used for the ultrashort excitation of the fluorescent molecules is focused inside the spray using a long-distance microscope lens to obtain two-photon absorption within a small volume of a few tens of microns. The out-of-field fluorescence usually observed in dense sprays when one-photon absorption is suppressed using this approach.

In a second step, both the temperature and the mixing fraction are measured seeding the two sprays by rhodamine B only. The decay is further examined to determine the lifetime of both sprays and the weight of the signal in the whole fluorescence signal. Results show that the volume fraction of a given spray must exceed about 10% to make it possible to determine its temperature and its volume fraction with a reasonable accuracy (typically a few percent for the volume fraction and 2°C for the temperature). Simultaneous measurements of the two sprays temperatures and volume fractions provides a means to calculate the mixing temperature (the average between the temperatures of the two sprays weighted by their volume fractions). One of the benefits of the newly developed technique is to remove the problem inherent to intensity-based measurements for evaluating the mixing temperature.

1. Introduction

The characterization of the droplet temperature in polydisperse sprays is an important challenge in many engineering applications. The transient phenomena within droplets that are heating or cooling, have long been the subjects of intense research in liquid fuelled combustion systems, spray cooling, spray drying, and many more processes related to sprays and liquid atomization in general. While the size and velocity of droplets can be measured using relatively widespread and well-established techniques, characterizing the temperature is less straightforward (Lemoine & Castanet, 2013). Several approaches relying upon a wide variety of physical principles have been brought in the recent decades and are still being actively pursued, like rainbow refractometry (Lemaitre et al., 2006; Saengkaew et al., 2018), Raman scattering (Carns et al., 1990; Müller et al., 2000; Schweiger, 1990), IR thermography (Brutin et al., 2011; Tuckermann et al., 2005), and laser-induced photoluminescence processes including laser-induced fluorescence (Lemoine & Castanet, 2013) and laser-induced phosphorescence (Strizhak et al., 2020). Among these techniques, laser-induced fluorescence (LIF) offers unprecedent temperature sensitivities and a high flexibility for a wide range of applications. Examples include droplets spreading onto solid surfaces(Chaze et al., 2017), mono and multi-component fuel droplets combusting and evaporating in high-temperature environments (Perrin et al., 2015), supercooled droplets in icing processes (Stiti et al., 2019). Usually, an organic dye is dissolved into the liquid prior to its injection. The droplets are illuminated by a laser beam with an appropriate wavelength to allow light absorption by the fluorescent molecules which emit in return a fluorescence signal depending on the temperature by some of its properties (intensity, wavelength, lifetime). A few dyes, such as rhodamine B or kiton red, have been used so far for measuring the temperature in water solutions.

LIF-based temperature measurements in both single or multiphase flows are usually based on the intensity of the fluorescence signal. However, intensity measurements cannot provide an absolute quantity. A reference, measured at a point where the temperature is already known, is always required. Any disturbance (in the intensity of the light source, in the background light, in the light transmission through the detection optics, or due to the dye photo-bleaching and degradation) will lead to some errors in the derived temperature. In sprays, it is generally unavoidable to use a ratiometric approach, i.e., to calculate the ratio of the intensities of the fluorescence signal collected in two spectral bands. Properly used, intensity ratios can cancel out most of the adverse effects encountered with droplets and thus provide the basis for accurate droplet temperature

measurements in droplet laden flows (Castanet et al., 2003, 2016; A Labergue et al., 2017; Stiti et al., 2019). Nonetheless, in spray applications, several sources of error have been reported (A. Labergue et al., 2010, 2012) due to the polydispersion in droplet size and multiple light scattering by the droplets. In particular, light scattering by the droplets of the laser beam can induce a significant out-of-field fluorescence, which extends outside the focal plane of the collection optics and contributes to the overall fluorescence signal. Droplets normally localized well outside the laser beam emit a substantial amount of parasitic fluorescence because of laser light scattering. Problems related to the achromaticity of the optics with the depth of field are thus becoming critical (A. Labergue et al., 2010, 2012). Intensity-based measurements are usually limited by the dynamic range of their detectors, which are not able to detect with the same settings (gain voltage, laser power…) individual droplets when they have very different size. The larger drops are generally more prominently represented in the average temperature, while the signal from the smaller drops falls to about the same level as the noise and is discarded in the acquisition processing.

In a recent study (Mehdi et al., 2021), we proposed a new method of measurements of the temperature based on the fluorescence lifetime. Contrary the fluorescence intensity, the lifetime value is not dependent on the measurement method and system. It also is closely dependent on the quenching rate of the fluorescence and therefore on the temperature. The Time Correlated Single-Photon Counting method (TCSPC) was employed to measure the temperature of water droplets in a polydisperse spray. Although the technique is not suitable for measuring the temperature of individual droplets, it was possible to obtain the average volume temperature of the liquid phase with limited measurement errors. The TCSPC technique operates on single photons regardless of their origin (large or small droplets), which makes it possible to characterize the average temperature of the droplets with a higher degree of accuracy. Due to the very high signal-to-noise ratio, measurements were also possible in the low-density spray regions.

The present work is built upon this previous effort to improve temperature measurement in sprays. Compared to this previous work, a two-photon excitation of fluorescent molecules is implemented. A key benefit of two-photon absorption is its ability to restrict the fluorescence excitation to a tiny focal volume around the laser beamwaist. The effects of scattering suffered by the excitation beam in sprays are mitigated, since photons undergoing multiple scattering processes, spread in space and time with a very low probability of having two-photon simultaneously absorbed. The technique is applied here to the mixing of two sprays, one hot and one cold. The aim of the present study is not only to measure the temperature in this situation of spray mixing, but also to show that the characterization of the fluorescence decay in the time domain can extend the capabilities of measurement to the mixing fraction and the temperature of the two individual sprays.

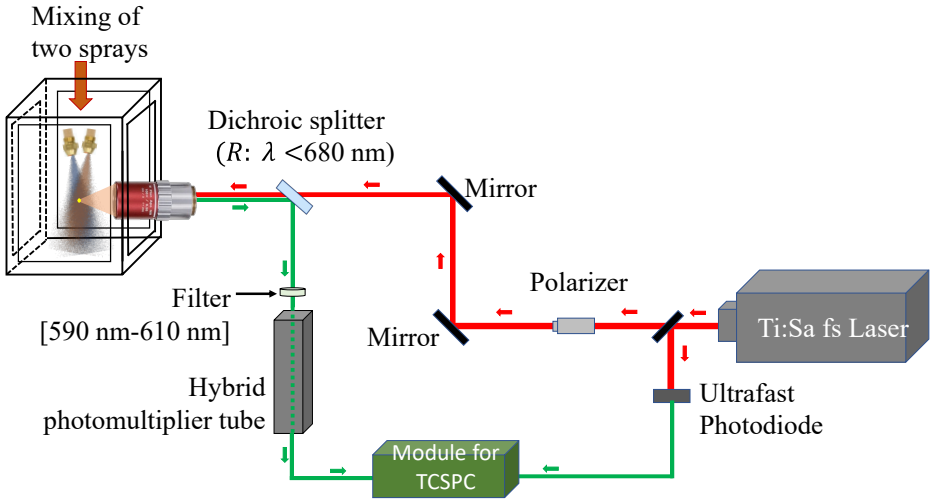

Fig. 1: Experimental setup.

Two-photon excitation

In this work, the simultaneous absorption of two photons is used in order to excite the fluorescent molecules from the ground state energy to the excited state. Several fluorescent dyes including rhodamine B, Eosin Y and rhodamine 6G are dissolved into water to conduct the experiments. The excitation of these fluorescent dyes is performed by a femtosecond Ti:Sapphire laser (Coherent Chameleon Ultra II) whose emission wavelength is tunable from 690 to 1080 nm and generates light pulses with a width of about 140 fs. To perform the experiments with rhodamine B, the fs laser is tuned on the wavelength of 800 nm at which the output power is 3.8 W. For eosin Y, a wavelength of 700 nm was preferred as it is more efficiently absorbed. The laser beam is focused by means of a microscope objective with a long working distance of 25 mm (50X Mitutoyo Corrected Infinite Plane Apo NIR B). The same objective is also used for collecting the emitted fluorescent photons. A fine observation in a cuvette shows that the two-photon fluorescence spot is restricted to a region of about 250 µm x 20 µm x 20 µm at the maximum laser output power.

Since absorption depends on the simultaneous absorption of two photons, its probability is proportional to the square of the laser light intensity I. Considering a small volume V, illuminated by a laser beam of intensity I, the number of photons absorbed N_{abs} can be written as:

$$N_{abs} \sim \delta\, C\, I^2 V \qquad (1)$$

In this expression, δ denotes the molecular two-photon absorption cross-section of the fluorophores in the liquid solution. It is usually quoted in (GM), where 1 GM is 10^{-50} cm^4 s photon^{-1}. The absorption volume V depends on the laser light fluence, and thus on the laser focalization. It can be adjusted in practice to limit the measurement volume to only a few microns. This, however, comes with a reduced fluorescence signal, especially due to a lower probability of intercepting a droplet.

Fluorescence lifetime measurements in the time domain

After an excitation by an ultrashort pulse of light, fluorescent molecules emit a signal that can be written as followed:

$$F(t) = \frac{1}{2}\,\phi(t)\,\eta\,N_{abs} \quad (2)$$

Here η is related to the collection efficiency of the measurement system. Fluorescence typically follows a first-order kinetics. The term $\phi(t)$ expresses the fluorescence decay resulting from the progressive decrease of the number of molecules in the excited state. In general, it follows a monoexponential distribution:

$$F(t)/F(t=0) = \mathrm{e}^{-t/\tau}, \quad (3)$$

where τ is the fluorescence lifetime, which is on the order a few nanoseconds for organic dyes such as rhodamine B, eosin Y and rhodamine 6G considered in the present study. In the literature, biexponential decays were sometimes used to describe the decay of some fluorophores including rhodamine B (Boens et al., 2007; Kristoffersen et al., 2014; Mehdi et al., 2021). In this case, the decay can be described using the following expression:

$$F(t)/F(t=0) = a\,\mathrm{e}^{-\frac{t}{\tau_1}} + (1-a)\,\mathrm{e}^{-\frac{t}{\tau_2}}, \quad (4)$$

where a is a parameter between 0 and 1. An average fluorescence lifetime τ for this type of decay can be computed as (Casadevall I Solvas et al., 2010):

$$\tau = a\,\tau_1 + (1-a)\,\tau_2, \quad (5)$$

The rate of non-radiative pathways k_{nr} and radiative pathways k_f modifies the number of molecules in the excited state. The total decay rate τ is the sum over all the radiative and non-radiative decays rate:

$$\tau = \left(k_f + k_{nr}\right)^{-1}. \quad (6)$$

The fluorescence lifetime depends on solvent effects through the non-radiative rate constant k_{nr}. Effects of the solvent include a dynamic contribution caused by collisions with the solvent molecules and a static contribution arising from short-range chemical interactions. An Arrhenius law has been widely accepted to describe the effect of temperature on the rate of the non-radiative decay for many solvents like rhodamine B (Mendels et al., 2008). For simplicity, this law is also considered for the temperature dependence of the fluorescence lifetime (Mendels et al., 2008; Mercadé-Prieto et al., 2017) :

$$\tau = A\,\exp\left(\frac{E_a}{RT}\right), \quad (7)$$

where E_a is the activation energy, A is a pre-exponential factor and R is the gas constant ($R = 8.314\ \mathrm{J.K^{-1}.mol^{-1}}$).

To characterize the fluorescence decay, the TCSPC (Time Correlated Single Photon Counting) technique is used. A fast hybrid photomultiplier tube (R10467, Hamamatsu) with a Peltier cooler to reduce the dark count rate, is used for photon counting. The output of the detector is sent to a time-correlating counter (HydraHarp 400 controller, PicoQuant GmbH) which is operating in

forward start stop mode to measure the arrival times of single photons. A laser pulse causes a photon event at the detector and the electronics measures the delay between the laser pulse and the subsequent photon event. This measurement implies a sharp timing of the laser pulse, which is obtained from a fast photodiode (TDA 200 from PicoQuant GmbH) connected to the timing electronics. This photodiode receives the reflected light from a beam splitter (99% T, 1% R) placed at the laser output and allows detecting the laser pulses with a small-time jitter due to a very sharp falling edge (Fall time typ. 250 ps). The fluorescence signal is collected by the same objective lens used to focus the laser beam. The fluorescence signal is diverted by a dichroic plate towards to a fast hybrid photomultiplier tube (R10467 from Hamamatsu) sensitive to single photon. A bandpass filter [590 nm - 610 nm] is placed in front of the photomultiplier tube to limit the detection of unwanted photons. The *basic* principles of TCSPC have been discussed with *great* details in the literature (Lakowicz, 2013). The measurement method illustrated in Figure 2, is based on the repetitive and precisely timed registration of single photons using the previously described system. By *counting* a high number of photon events to achieve statistical convergence, a *histogram* of the photon arrival times distribution can be built up. The width of the time bins in this histogram depends on the required time resolution (typically a few tens of ps).

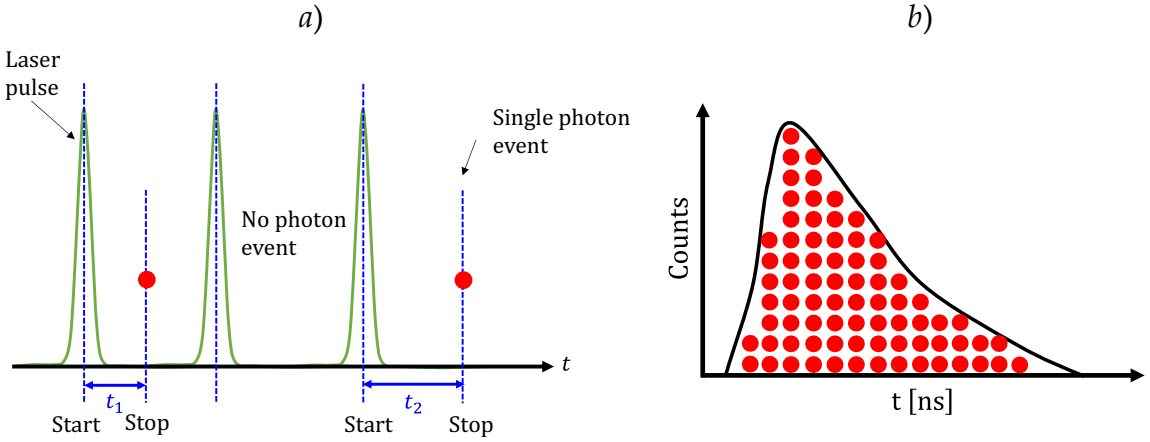

Fig. 2: The principle of the lifetime measurement with TCSPC. a) the TCSPC device typically measures the time between one START event and one STOP event (like a stopwatch). b) A histogram of start-stop times is reconstructed by counting a high number of photon events to reach statistical convergence.

A non-linear least squares analysis is used to test if the model is consistent with the data and estimate the parameters of the fluorescence decay model. Basically, parameters are varying until the goodness-of-fit parameter χ^2 determined by:

$$\chi^2 = \frac{1}{n}\sum_{k=1}^{n}\frac{\left(N(t_k)-N_c(t_k)\right)^2}{N(t_k)}, \qquad (8)$$

In the above expression, $N(t_k)$ is the measured counts at time t_k, $N_c(t_k)$ is the modeled number of counts at time t_k assuming a mono (Equation 3) or a biexponential (Equation 4) function for the fluorescence decay, and n is the number of data points. A good fit is characterized by a value of χ^2close to 1 and the weighted residual between the measured and calculated decay curves randomly distributed around 0.

Temperature calibration

Before measuring the droplet temperature in a spray, it is necessary to perform a calibration of the fluorescence lifetime as a function of temperature. The fluorescence lifetime is measured in a cell for different temperatures. The liquid is heated by means of a thermal resistance while it is continuously stirred to ensure a uniform temperature. A thermocouple is positioned a few mm from the LIF measurement volume. Figure 3 shows the fluorescence decay of rhodamine B for different temperatures in the considered detection band. Since the mono-exponential character of the fluorescence decay is not perfect and evolves with the temperature. It is preferred to use the average lifetime τ, calculated by Equation (5), as an indicator of the temperature of the liquid, rather than τ_1, τ_2 and a_1. Figure 4 shows the evolution of the lifetime τ in function of the temperature for the three fluorescent dyes. As observed, Rhodamine 6G has a long lifetime of approximately 3.8 ns, which is not sensitive to temperature as already noticed by (Chaze et al., 2017) Eosin Y has a short lifetime of about 1.1 ns whose temperature variation is very weak. Based on Equation (7), the activation energy E_a and the parameter A can be evaluated from the curve presented in Figure 4. In the case of rhodamine B, this leads to E_a=19.890 kJ/mol and $A = 4.852 \cdot 10^{-4}\ s$. In Figure 5, a careful observation of the fluorescence decays shows that Rhodamine 6G exhibits a monoexponential decay, while Eosin Y and rhodamine B have a slightly biexponential decay.

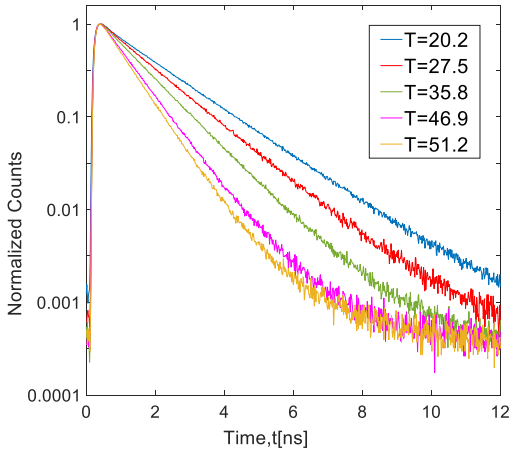

Fig. 3: Fluorescence decay of Rhodamine B at different temperatures.

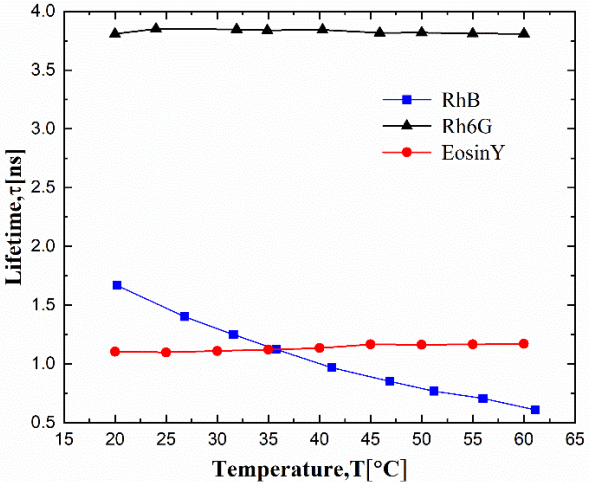

Fig. 4: Effect of the temperature on the average fluorescence lifetimes of rhodamine B, Eosin Y and rhodamine 6G

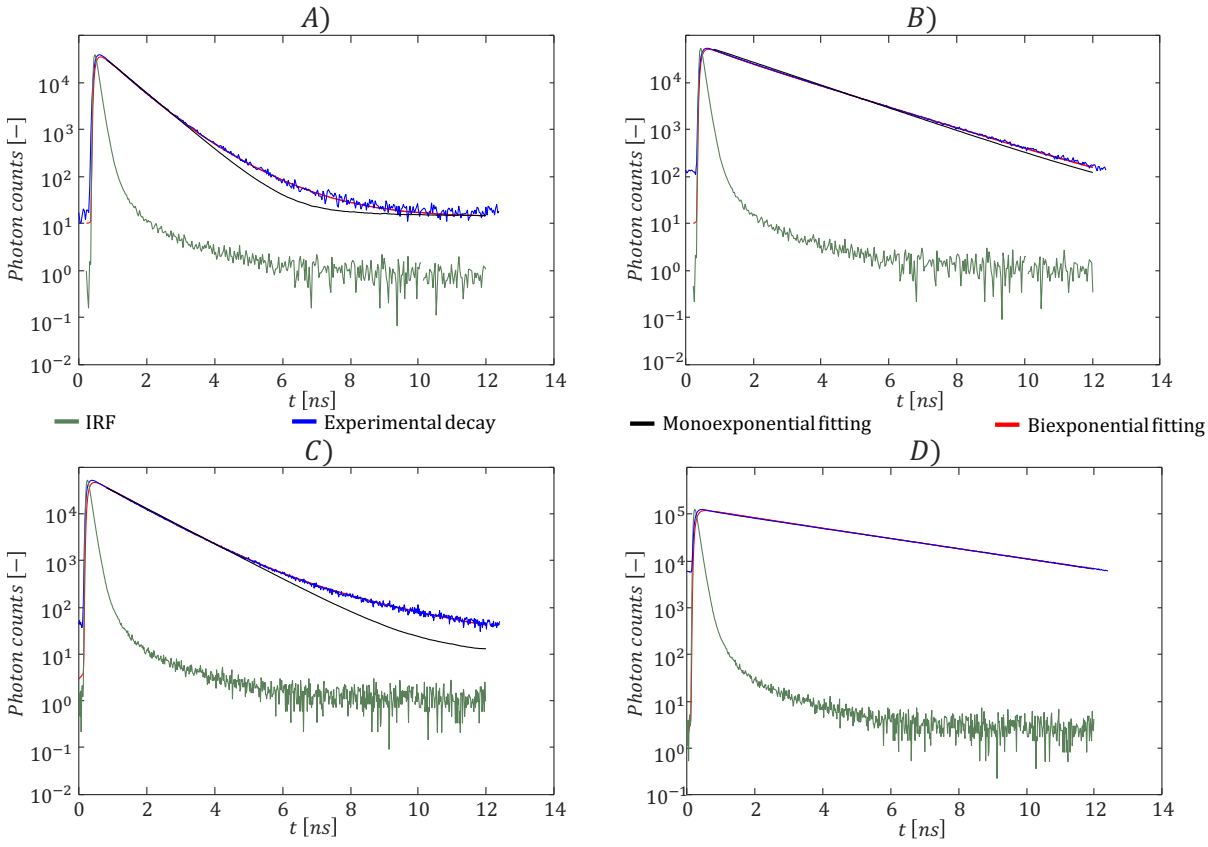

Fig. 5: Fluorescence decays of rhodamine B at 60°C (A) and 19°C (B), eosin Y at 20°C (C) and rhodamine 6G at 20°C (D). Fitting by monoexponential and biexponential functions.

Application to temperature measurement in sprays

The experimental system allows to generate two *full cone spray*s downward with an adjustable tilt angle (Figure 6). The two sprays are produced by a pressure swirled atomizer (Danfoss oil nozzle, angle 30° type S, 0.65 USgal/h). Indications about the size and velocity distributions of the droplets can be found in the study by Labergue et al. (A. Labergue et al., 2012) using the well-established Phase Doppler technique to obtain joint size/velocity PDFs. The liquid flows across a heat exchanger, which allows to control the liquid temperature in the nozzle. The temperature of the two sprays can be adjusted independently. A K-type thermocouple inserted in the inlet pipe of each nozzle, is used to determine the injection temperature of the sprays. The spraying system is mounted on translations stages which allows moving the two sprays relatively to the optics and perform measurements at different positions. At an inlet pressure of 6 bar, the droplet mean diameter D_{10} is roughly 20 μm, while the droplet density is of the order of 5.10^4 particles per cm^3 (at about 1 cm after the breakup zone). The probability of collision between two droplets originating from the two sprays is very low (Alexandre Labergue et al., 2013). There are practically no droplets formed from the merging of droplets of the two sprays. The interaction between the sprays is expected to occur mostly via the air entrained by each spray and the subsequent convective heat transfer. In the measurement volume where the two-photon absorption process takes place, fluorescence is emitted by the droplets of the two sprays. Two distinctives fluorescence decays from these droplets are encountered in the following situations:

1) The temperatures of the two sprays are different and a temperature-dependent dye (like rhodamine B) is used.
2) The two sprays are seeded with two dyes having significantly different fluorescence lifetimes like Eosin Y and rhodamine 6G.

These two situations will be examined in the following to study the mixing of non-isothermal sprays.

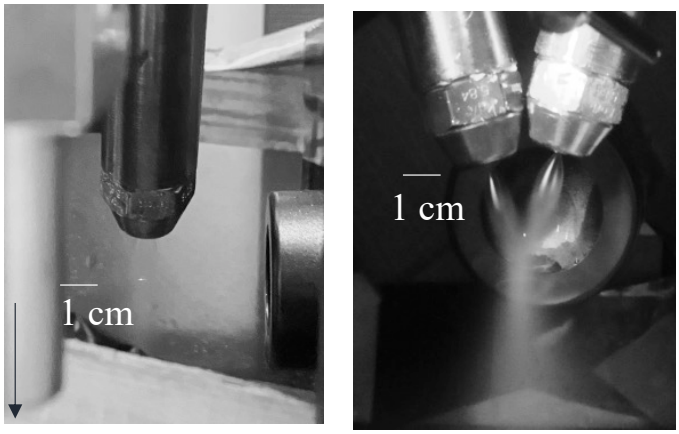

Fig. 6: Side view of the mixing sprays. The biphotonic fluorescence corresponds to the bright spot observed in the middle of the spray region.

Fluorescence signal in the mixing zone

In this section, it is assumed that the two sprays are seeded with a dye that has a monoexponential decay. A volume V_1 of liquid coming from the first spray and V_2 of the second spray are crossing the measurement volume during the acquisition of the fluorescence signal. According to Equations (1-3), the detected fluorescence signal is expected to have the following time evolution:

$$F(t) = \eta\ \delta_1\ C_1\ I^2 \exp\left(-\frac{t}{\tau_1}\right) V_1 + \eta\ \delta_2\ C_2\ I^2 \exp\left(-\frac{t}{\tau_2}\right) V_2. \quad (9)$$

Normalizing the signal by $F(t=0)$, the previous evolution can be rewritten as follows:

$$\frac{F(t)}{F(t=0)} = a \exp\left(-\frac{t}{\tau_1}\right) + (1-a) \exp\left(-\frac{t}{\tau_2}\right), \quad (10)$$

where the average coefficient a is given by:

$$a = \frac{\delta_1\ V_1 C_1}{\delta_1\ V_1 C_1 + \delta_2\ V_2 C_2}. \quad (11)$$

Introducing the mixing fraction $\psi = \frac{V_1}{V_1 + V_2}$:

$$a = \frac{\psi}{\psi + \beta\ (1-\psi)}, \quad (12)$$

where $\beta = \delta_1 C_1 / \delta_2 C_2$. The latter expression establishes a relationship between the mixing fraction ψ and the average coefficient a which can be obtained by an interpolation of the experimental fluorescence decay by a biexponential curve (Equation 10). If sufficiently accurate, measurements should make it possible to evaluate the parameters a, τ_1 and τ_2 in Equation (10). Hence, it seems feasible to measure at the same time, the mixing fraction ψ, and the individual temperature of the two sprays (namely T_1 and T_2) given by the values of τ_1 and τ_2. This analysis also makes it possible to determine the fluorometric temperature T_{LIF} defined from the average lifetime $\bar{\tau}$:

$$\bar{\tau} = a\ \tau_1 + (1-a)\ \tau_2 \text{ and } T_{LIF} = \frac{R}{E_a} \cdot ln(\bar{\tau}/A) \cdot \quad (13)$$

Even when $\beta = 1$, the temperature T_{LIF} differs from the mixing temperature T_m given by the conservation of energy and the mixing fraction ψ:

$$T_m = \psi\ T_1 + (1-\psi)\ T_2. \quad (14)$$

In the general case, however, the fluorescence decay in the two sprays differ from a monoexponential decay but can be modelled by a biexponential decay (Figure 5). In this situation, the measurement principle described above remains mostly valid, but Equation (9) must be rewritten as:

$$F(t) = \eta\ \delta_1\ C_1\ I^2\ \phi_1(a_1, t_{11}, t_{12}, t)\ V_1 + \eta\ \delta_2\ C_2\ I^2\ \phi_2(a_2, t_{21}, t_{22}, t) V_2, \quad (15)$$

where $\phi_1(a, t_1, t_2, t) = a \exp(-t/t_1) + (1-a) \exp(-t/t_2)$ and $0 \leq a_{1,2} \leq 1$.

Parameters (a_1, t_{11}, t_{12}) for spray 1, and (a_2, t_{21}, t_{22}) for spray 2, must be determined prior to the measurements by a temperature calibration, as they can vary with the temperature in a rather complex manner. Normalizing the signal in Equation (15) by $F(t=0)$,

$$\frac{F(t)}{F(t=0)} = a\,\phi_1(a_1, t_{11}, t_{12}, t) + (1-a)\,\phi_2(a_2, t_{21}, t_{22}, t). \qquad (16)$$

Finally, the temperature in the two respective sprays, as well as the average coefficient a can be adjusted with the least squares method (Equation 8) in the mixing region of the sprays.

Measurement of the mixing fraction alone

To illustrate the principle of measuring the mixing fraction ψ, the previous model is applied to the mixture of a hot liquid spray injected at 60°C and a liquid spray at room temperature (19°C). The hot spray is seeded with Rhodamine 6G and the cold spray with Eosin Y. The low temperature dependence of the lifetime of both dyes allows fixing τ_1=3.8 ns and τ_2=1.1 ns in Equation (10). The least squares method (Equation 8) is then used to determine the value of a alone. The emission wavelength of the femtosecond laser was set at 700 nm and the output laser power at 1.5 W. Although the eosin Y decay is not purely monoexponential, the use of Equation (10) gives good results provided a calibration. Since the absorption cross-section δ_1 and δ_2 are unknown for rhodamine 6G and eosin Y, a calibration is necessary to establish a link between the average coefficient a and the mixing fraction ψ. This calibration is carried out in a cell where the two dyes are mixed in a perfectly controlled proportion. Figure 7 shows the fluorescence decay observed for several values of ψ between 0 and 1 using for the concentrations of the solutions before the mixing C_{Rh6G}=3 × 10^{-6}mol/L and C_{EY} =10^{-5} mol/L.

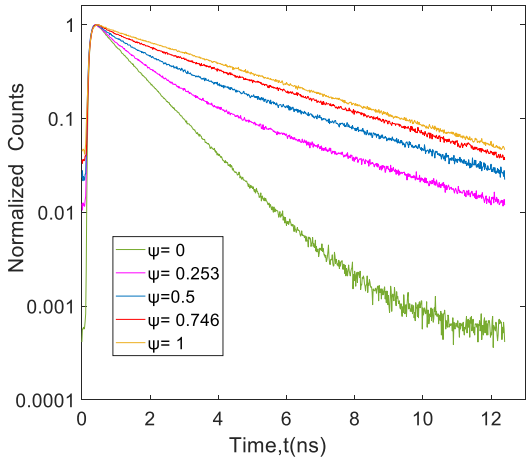

Fig. 7: Fluorescence decay of the couple rhodamine 6G/eosin Y when mixed in different proportions. These results were obtained in a cuvette at room temperature of 20°C (ψ=0 when there is no rhodamine 6G in solution)

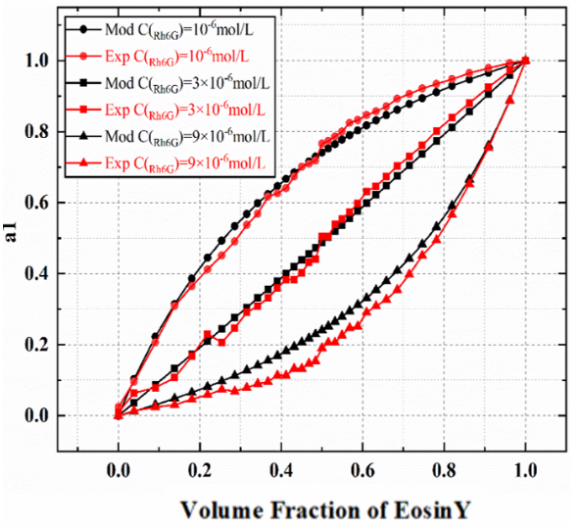

Fig. 8: Evolution of the average coefficient a as a function of the mixing fraction ψ for different concentrations of rhodamine 6G and eosin Y. The experimental data (in black) are compared to the prediction of Equation (12) (in red) adjusting β to 0.35, 1.05 and 3.15. Measurements correspond to a concentration of rhodamine 6G equal to 10^{-6} mol/L, 3×10^{-6}mol/L and 9×10^{-6} mol/L, while the concentration of Eosin Y is fixed at 10^{-5} mol/L.

Figure 8 shows the calibration curves obtained for three concentration ratios C_1/C_2=0.1, 0.3 and 0.9. An acceptable agreement with the prediction of Equation (12) is obtained by adjusting the value of β to 0.35, 1.05 and 3.15. From these results, it can be deduced that the ratio of the two-photon absorption cross sections δ_1/δ_2 of rhodamine 6G and eosin Y is approximately equal to 3.5 at an excitation wavelength of 700 nm.

For the measurements conducted in the spray, the following concentrations $C_1 = 3 \times 10^{-6}$ mol/L and $C_2 = 10^{-5}$ mol/L, were chosen for rhodamine 6G and eosin Y respectively. In these conditions, $\beta = 1.05$ and the average coefficient a is almost equal to the mixing fraction ψ. For the measurements, the spraying system (the nozzles and the mixing chamber) are shifted by two motorized moving stages relatively to the microscope objective by steps of 0.5 mm in the x and z directions. An acquisition time of 30 s is applied at each measurement location, which proved more than sufficient to ensure a converged histogram of the fluorescence decay and assess the value of the mixing fraction a with an accuracy of the order of 0.5 %. A map of the ψ distribution is finally constructed to obtain a 2D image of the mixing fraction in the mixing region of the two sprays as shown in Figure 9. Since the two sprays are identical in this experiment and perfectly aligned, a mixing fraction equal to 0.5 can be found in the center of the mixing region. A left/right symmetric distribution of the mixing fraction is also observed when the two sprays cross each other and emerge diagonally on the opposite side.

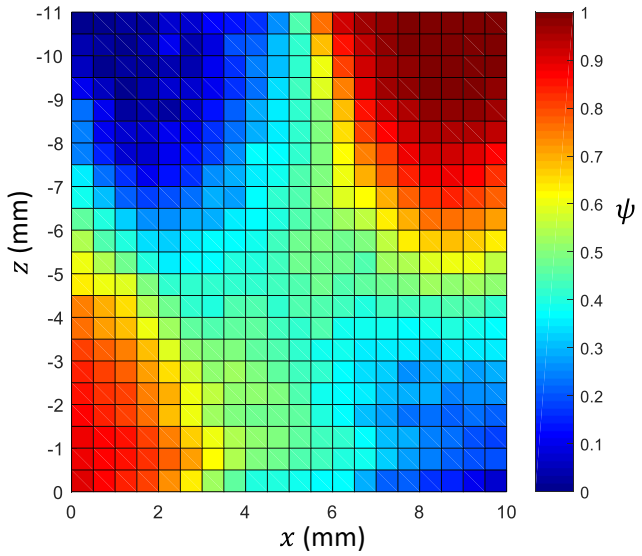

Fig. 9: Distribution of the mixing fraction ψ in the mixing region of the two sprays. The liquid flow rate of the two sprays is about 0.6 L/min.

Measurement of both the mixing fraction and the temperatures of the two sprays

An even more valuable type of measurement is the combined determination of the temperatures of the two sprays and the mixing fraction. This type of measurement can be achieved by using rhodamine B as a unique fluorescent dye. As the absorption cross-section of rhodamine B is not dependent on temperature, the value of β is equal to 1 in Equation (12) which means $a = \psi$. An accurate assessment of a, t_1 and t_2 requires having a sufficient sensitivity to the three parameters which implies a sufficiently high temperature difference between the sprays. In the present work, the injection temperature of spray 1 is set to 19°C and that of spray 2 is 59°C. To ensure a good data convergence, the acquisition time was fixed at 100 s. In addition, measurement points are excluded from the data processing at locations where the count rate of the photons is below 2000 cps. These measurements are feasible in principle given the noise level (around 30 cps), but they would require more time of acquisition for a good statistical convergence.

As mentioned earlier, the fluorescence decay of rhodamine B deviates significantly from a monoexponential, but it can be very well described by a biexponential (Figure 5). If this behavior is not considered, the value of the average coefficient a obtained from a biexponential fitting (Equation 10) can lead to an erroneous evaluation of the mixing fraction ψ as illustrated in Figure 10.A. Indeed, it is apparent on this figure that the value of a never falls below 0.22, even when there is only one spray in the measurement volume (presently, a is about 0.22 for the coldest spray).

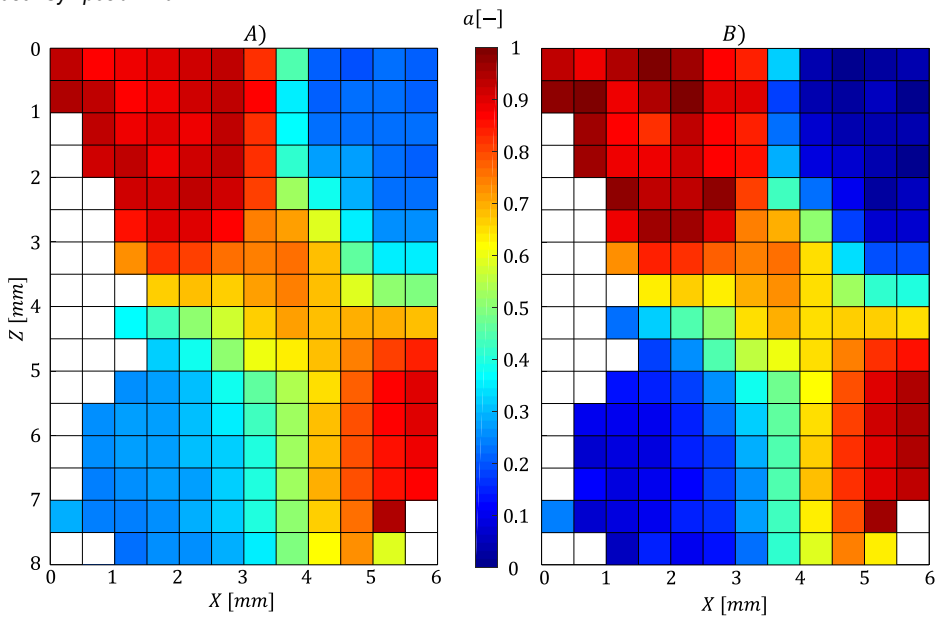

Fig. 10: Spatial distribution of the average coefficient a. The values are obtained by assuming either a biexponential decay (A) based on Equation 10, or the composition of two biexponential decays (B) based on Equation 18.

To avoid this problem, the chosen approach is to search for the best combination of two biexponentials (Equation 16) among those observed for rhodamine B at different temperatures in a cuvette or in a single spray (no mixing). From these experiments, it was determined that the biexponential decay of rhodamine B can be well described using the following formula:

$$\phi(a, t_1, t_2, t) = a \exp(-t/t_1) + (1-a) \exp(-t/t_2) \qquad (17)$$

where $a = 0.9901 \cdot 10^{-1} \cdot \bar{\tau}(ns) + 0.04371$, $t_2(ns) = -0.411765 \cdot \bar{\tau}(ns) + 1.4594$ and $\bar{\tau} = a \cdot t_1 + (1-a) \cdot t_2$. These correlations are valid in the range 0.6 ns $\leq \bar{\tau} \leq$ 2 ns.

Finally, considering the averaged lifetime $\bar{\tau_1}$ and $\bar{\tau_2}$ in the two sprays, the fluorescence signal in the mixing regions can be written:

$$\frac{F(t)}{F(t=0)} = a\, \phi_1(\bar{\tau_1}, t) + (1-a)\, \phi_2(\bar{\tau_2}, t). \qquad (18)$$

The introduced data processing aims to find the triplet (a, $\bar{\tau_1}$, $\bar{\tau_2}$) using the least squares method, i.e. minimizing the value of χ^2 in Equation (8). By adopting this method, the new distribution of the coefficient a shown in Figure 10.B, is much more acceptable for the mixing fraction ψ with values extended to 0 and 1 in the regions where the two sprays are separated.

From the extracted values of ψ, T_1 and T_2, it is possible to calculate the mixing temperature T_m based on Equation (14). As observed in Figure 11.A, the hot spray (T_{inj} = 59°C) appears to get slightly cooler after the mixing, while the cold spray (T_{inj} = 19°C) appears to be heated up by a

few °C. Figure 11.B shows the evolution of the mixing fraction ψ along the diagonal lines passing through the axis of the two sprays which are plotted in gray in Figure 11.A. As expected, the value of ψ approaches 1 in the hot spray region and 0 in the cold spray region but a deviation (about 5%) is sometimes observed. Between $z = 2$ mm and $z = 5$ mm, ψ is varying due to the mixing of the sprays. It is decreasing for the hot spray diagonal down to about 0.65, while it increases for the cold spray diagonal up to about 0.7. After the mixing zone ($z > 5$ mm), only one spray remains in the measurement volume. The fraction ψ returns a value close to its initial, although the observed values of ψ suggest that residual of droplets from the other spray may remain but in a very weak quantity.

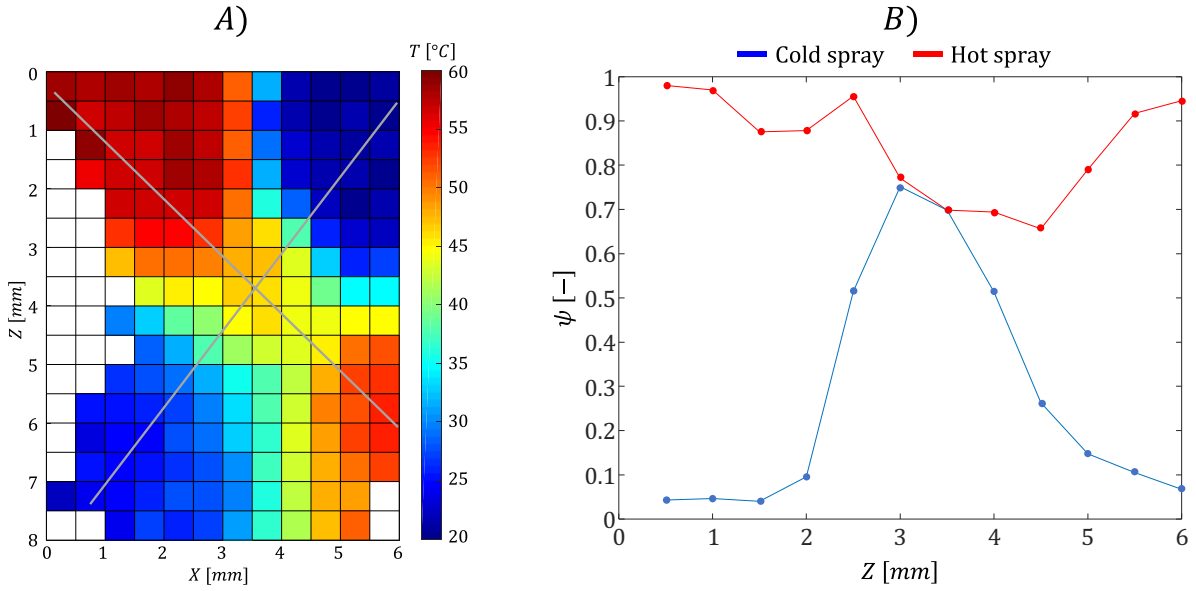

Fig. 11: A) Spatial distribution of the mixing temperature T_m based on Equation 13. The two gray lines correspond to the diagonals passing through the axis of the two sprays. B) represents the evolution of the mixing fraction as a function of the vertical position z.

Figure 12 A and B shows the evolution of the temperature in the hot and cold sprays (respectively T_1 and T_2), the temperature T_{LIF} derived from the average fluorescence lifetime (Equation 13) and the mixing temperature T_m based on Equation (14) as a function of the vertical position z on the hot and cold spray diagonals respectively. It should be noted that the temperature T_m is systematically a few degrees higher than the temperature T_{LIF}, and the largest differences are observed in the mixing zone. In Figure 12 A for $z < 2$ mm, since T_1 and T_2 are close to 60°C, there is no ambiguity on the fact that there is in fact a single spray. When spray 2 (cold spray) is present in sufficient quantity (in the mixing zone), the temperature T_2 takes a value close to 20°C, which is comparable to the injection temperature of the cold spray. After the mixing zone ($z > 5$ mm), only

the hot spray remains in the measurement volume, and it is observed that the temperature T_1 of the hot spray has slightly decreased from the injection temperature. Similar conclusions can be drawn in Figure 11 B for the results obtained along the axis of the cold spray.

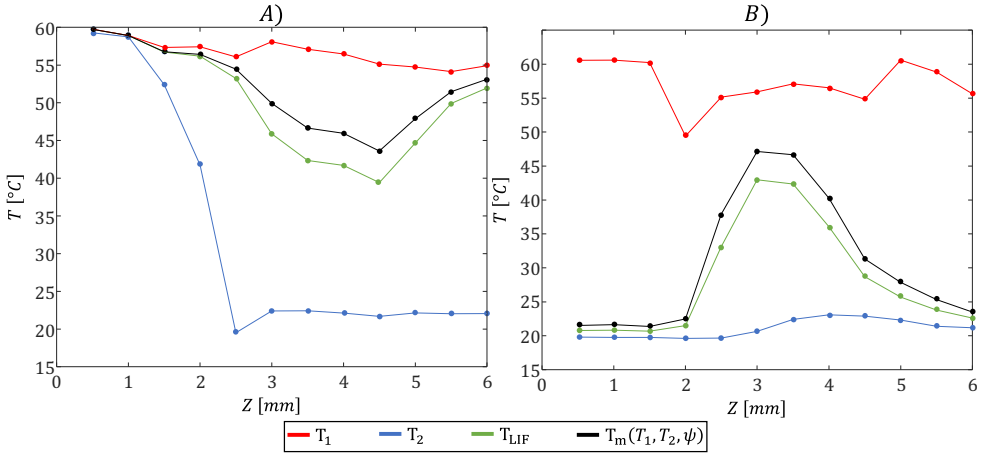

Fig. 12: Evolution of the LIF temperature T_{LIF}, mixing temperature T_m and temperature of both hot T_1 and cold spray T_2 as a function of the vertical position for A) the hot spray diagonal and B) the cold spray diagonal plotted in Figure 11A.

Even if the temperatures T_1 and T_2 of both sprays is reasonably well recovered in Figure 12, the measurement method suffers from limitations when one of the sprays is weakly present in the measurement volume. In this case, the temperature of the weakly present spray cannot be reliably determined. Figure 13 provides an indication of the accuracy of the temperature measurements of both sprays (T_1 and T_2). In Figure 13A, the measurement position is situated in a region of the cold spray is dominant ($x = 1.5$ mm and $z = 7$ mm). It is evidenced that the temperature T_1 of the hot spray can be changed in a large range while correctly fitting the experimental fluorescence decay with the model based on Equation (18). The confidence interval for the hot spray temperature T_1 extends from about 44°C to 72°C. In contrast, the temperature T_2 of the cold spray ranges between 21°C and 22.5°C, which is acceptable for a measurement accuracy. Further calculations would demonstrate that T_m and T_{LIF} are measured with an accuracy better than 1°C even when T_1 is measured with the largest admissible error. This means that both T_m and T_{LIF} can still be measured correctly although the mixing fraction, T_1 or T_2 are significantly wrong.

Figure 13B corresponds to a position in the center of the mixing zone, where the volume fraction of the two sprays is comparable ($x = 1.5$ mm and $z = 3.5$ mm). It is apparent, that both temperatures T_1 and T_2, as well as the mixing fraction ψ, are estimated with a good accuracy in that case.

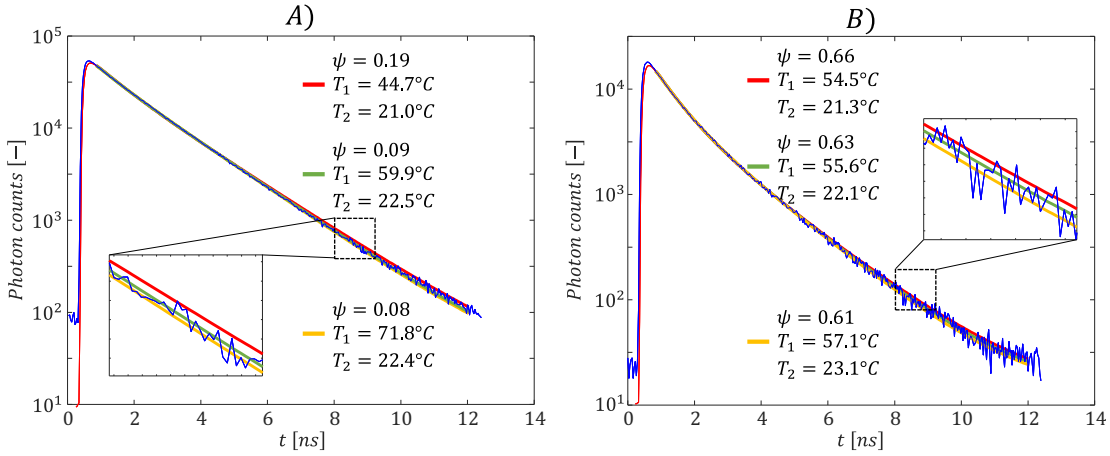

Fig. 13: Estimation of the hot T_1 and cold temperature T_2 in a region where A) the cold spray is in the majority A) ($x = 1.5\,mm;\ z = 7\,mm$) and in the mixing region ($x = 1.5\,mm;\ z = 3.5\,mm$)

Conclusions

A new method for measuring the local temperature in sprays using the two-photon absorption is developed and tested. The method is based on the measurement of the fluorescence lifetime of certain dyes for which the fluorescence quantum yield is particularly sensitive to temperature such as rhodamine B. One of the major advantages of using the fluorescence lifetime relates to the fact that it is an intrinsic molecular property, which is not affected by fluctuations in excitation source intensity or in the collections of the fluorescence signal. Time-correlated single-photon counting (TCSPC) is particularly well suited to carry out temperature measurements because it is able to work with a high signal-to-noise ratio, while the measurement volume is reduced to a few tens of microns. Using TCSPC to study the mixing of two sprays is particularly interesting when the droplets of the two sprays fluoresce with a sufficiently different fluorescence lifetime. In such situation, the time decay of the fluorescence makes it possible to retrieve the temperature of the two sprays as well as their mixing fraction. The possibility of measuring the mixing fraction alone was first tested in the case of a mixture of two sprays seeded separately with eosin Y and rhodamine 6G, which have very different fluorescence lifetimes but both insensitive to temperature. The combined measurement of temperature and mixing fraction using rhodamine B alone, was carried out for a thermal contrast of approximately 40°C between the two sprays. The biexponential behavior of the fluorescence decay of rhodamine B must be considered to obtain acceptable values of the mixing fraction. It was found that the volume fraction of a spray must exceed about 10% to make it possible to derive its temperature with an acceptable accuracy of about 2°C-3°C. The mixing temperature based either on the average lifetime or on the mixing

fraction (mixing temperature weighted by the liquid volume of the sprays) are always accurately measured, although the two can differ by a few °C in the mixing zone.

References

Boens, N., Qin, W., Basarić, N., Hofkens, J., Ameloot, M., Pouget, J., Lefèvre, J. P., Valeur, B., Gratton, E., VandeVen, M., Silva, N. D., Engelborghs, Y., Willaert, K., Sillen, A., Rumbles, G., Phillips, D., Visser, A. J. W. G., Van Hoek, A., Lakowicz, J. R., … Miura, A. (2007). Fluorescence lifetime standards for time and frequency domain fluorescence spectroscopy. *Analytical Chemistry*. https://doi.org/10.1021/ac062160k

Brutin, D., Sobac, B., Rigollet, F., & Le Niliot, C. (2011). Infrared visualization of thermal motion inside a sessile drop deposited onto a heated surface. *Experimental Thermal and Fluid Science*, *35*(3), 521–530. https://doi.org/10.1016/j.expthermflusci.2010.12.004

Carns, J. C., Moncivais, G., & Brock, J. R. (1990). *Time-resolved Raman spectroscopy from reacting optically levitated microdroplets*. *29*(19), 2913–2918.

Casadevall I Solvas, X., Srisa-Art, M., Demello, A. J., & Edel, J. B. (2010). Mapping of fluidic mixing in microdroplets with 1 μs time resolution using fluorescence lifetime imaging. *Analytical Chemistry*, *82*(9), 3950–3956. https://doi.org/10.1021/ac100055g

Castanet, G., Lavieille, P., Lebouché, M., & Lemoine, F. (2003). Measurement of the temperature distribution within monodisperse combusting droplets in linear streams using two-color laser-induced fluorescence. *Experiments in Fluids*, *35*(6), 563–571. https://doi.org/10.1007/s00348-003-0702-1

Castanet, G., Perrin, L., Caballina, O., & Lemoine, F. (2016). Evaporation of closely-spaced interacting droplets arranged in a single row. *Int J Therm Sci*, *93*, 788–802. https://doi.org/10.1016/j.ijheatmasstransfer.2015.09.064

Chaze, W., Caballina, O., Castanet, G., & Lemoine, F. (2017). Spatially and temporally resolved measurements of the temperature inside droplets impinging on a hot solid surface. *Experiments in Fluids*, *58*(8). https://doi.org/10.1007/s00348-017-2375-1

Kristoffersen, A. S., Erga, S. R., Hamre, B., & Frette, Ø. (2014). Testing fluorescence lifetime standards using two-photon excitation and time-domain instrumentation: Rhodamine B, coumarin 6 and lucifer yellow. *Journal of Fluorescence*. https://doi.org/10.1007/s10895-014-1368-1

Labergue, A., Delconte, A., Castanet, G., & Lemoine, F. (2012). Study of the droplet size effect coupled with the laser light scattering in sprays for two-color LIF thermometry measurements. *Experiments in Fluids*, *52*(5), 1121–1132. https://doi.org/10.1007/s00348-011-1242-8

Labergue, A., Deprédurand, V., Delconte, A., Castanet, G., & Lemoine, F. (2010). New insight into two-color LIF thermometry applied to temperature measurements of droplets. *Experiments in Fluids*, *49*(2), 547–556. https://doi.org/10.1007/s00348-010-0828-x

Labergue, A, Pena-Carillo, J.-D., Gradeck, M., & Lemoine, F. (2017). Combined three-color LIF-PDA measurements and infrared thermography applied to the study of the spray impingement on a heated surface above the Leidenfrost regime. *International Journal of Heat*

and Mass Transfer, *104*, 1008–1021. https://doi.org/10.1016/j.ijheatmasstransfer.2016.07.029

Labergue, Alexandre, Delconte, A., & Lemoine, F. (2013). Study of the thermal mixing between two non-isothermal sprays using combined three-color LIF thermometry and phase Doppler analyzer. *Experiments in Fluids*, *54*(6), 1–15. https://doi.org/10.1007/s00348-013-1527-1

Lakowicz, J. R. (2013). *Principles of fluorescence spectroscopy*. Springer science & business media.

Lemaitre, P., Porcheron, E., Grehan, G., & Bouilloux, L. (2006). Development of a global rainbow refractometry technique to measure the temperature of spray droplets in a large containment vessel. *Measurement Science and Technology*, *17*(6), 1299–1306. https://doi.org/10.1088/0957-0233/17/6/002

Lemoine, F., & Castanet, G. (2013). Temperature and chemical composition of droplets by optical measurement techniques: a state-of-the-art review. *Experiments in Fluids*, *54*(7), 1572. https://doi.org/10.1007/s00348-013-1572-9

Mehdi, S., Yangpeng, L., Hadrien, C., Fabrice, L., Xishi, W., & Guillaume, C. (2021). Fluorescence lifetime measurements applied to the characterization of the droplet temperature in sprays. *Experiments in Fluids*, *62*(8). https://doi.org/10.1007/s00348-021-03264-x

Mendels, D. A., Graham, E. M., Magennis, S. W., Jones, A. C., & Mendels, F. (2008). Quantitative comparison of thermal and solutal transport in a T-mixer by FLIM and CFD. *Microfluidics and Nanofluidics*. https://doi.org/10.1007/s10404-008-0269-5

Mercadé-Prieto, R., Rodriguez-Rivera, L., & Chen, X. D. (2017). Fluorescence lifetime of Rhodamine B in aqueous solutions of polysaccharides and proteins as a function of viscosity and temperature. *Photochemical and Photobiological Sciences*. https://doi.org/10.1039/c7pp00330g

Müller, T., Grünefeld, G., & Beushausen, V. (2000). High-precision measurement of the temperature of methanol and ethanol droplets using spontaneous Raman scattering. *Applied Physics B*, *70*(1), 155–158.

Perrin, L., Castanet, G., & Lemoine, F. (2015). Characterization of the evaporation of interacting droplets using combined optical techniques. *Experiments in Fluids*, *56*(2). https://doi.org/10.1007/s00348-015-1900-3

Saengkaew, S., Godard, G., & Grehan, G. (2018). Global Rainbow Technique : Temperature evolution measurements of super-cold droplets. *ICLASS 2018, 14 Th Triennial International Conference on Liquid Atomization and Spray Systems, Chicago, IL, USA, July 22-26, 2018*, 1–7.

Schweiger, G. (1990). Raman scattering on single aerosol particles and on flowing aerosols: a review. *Journal of Aerosol Science*, *21*(4), 483–509.

Stiti, M., Labergue, A., Lemoine, F., Leclerc, S., & Stemmelen, D. (2019). Temperature measurement and state determination of supercooled droplets using laser-induced fluorescence. *Experiments in Fluids*, *60*(4), 1–13. https://doi.org/10.1007/s00348-018-2672-3

Strizhak, P. A., Volkov, R. S., Antonov, D. V., Castanet, G., & Sazhin, S. S. (2020). Application of the laser induced phosphorescence method to the analysis of temperature distribution in heated and evaporating droplets. *International Journal of Heat and Mass Transfer*. https://doi.org/10.1016/j.ijheatmasstransfer.2020.120421

Tuckermann, R., Bauerecker, S., & Cammenga, H. K. (2005). IR-thermography of evaporating acoustically levitated drops. *International Journal of Thermophysics*, *26*(5), 1583–1594.